Research Article

Isotopic Evidence for Long-term Bioaccumulation of Perfluoroalkyl Substances (PFASs) in Icelandic seabirds

Shen R.[1, *] Ebinghaus R.[1] Vassão D.[2] Ratcliffe N.[3] Larsen T[4]

1. Institute of Coastal Environmental Chemistry, Helmholtz Zentrum hereon, Geesthacht, Germany

2. Max Planck Institute for Chemical Ecology, Jena, Germany

3. British Antarctic Survey, Natural Environment Research Council, Cambridge, United Kingdom

4. Department of Archaeology, Max Planck Institute of Geoanthropology, Jena, Germany

*Corresponding author: Rui Shen rui.shen@studium.uni-hamburg.de

Abstract

Per- and polyfluoroalkyl substances (PFASs) are persistent anthropogenic pollutants with a widespread and significant impact on global marine ecosystems, particularly in the Arctic. Our study is centered in Iceland, an area where the merging of boreal and Arctic marine currents creates a complex ecological landscape. This setting is increasingly being influenced by the warming climate, adding another layer of complexity to the existing challenges posed by pollution. Focusing on two congeneric seabird species breeding in Iceland, the common guillemot (Uria aalge, UA), primarily a boreal species, and Brünnich's guillemot (Uria lomvia, UL), a true Arctic species, our research aims to monitor and understand the bioaccumulative behavior of PFASs. These seabirds, differing in ecological niches and migratory behaviors, serve as ideal sentinels for assessing the impacts of PFASs.

We collected blood plasma samples from both species (UA: n=67, UL: n=45) during their breeding season in June 2018 across Iceland. The analysis included PFASs measurement and stable isotopes of carbon (δ13C) and nitrogen (δ15N), offering insights into the seabirds' exposure levels and foraging behaviors, respectively. This dual-method approach provides a comprehensive assessment of how foraging patterns and past seasonal diet influence their PFASs exposure, shedding light on the ecological implications of these pollutants in the Arctic.

Our findings reveal the presence of C9-13 PFCAs and PFOS in all plasma samples, with a notable interspecies variation in exposure levels. Principal component analysis (PCA) indicates a bioaccumulative pattern predominantly driven by PFCAs homologues, highlighting PFOS persistence. UA generally showed higher exposure levels compared to UL (PFCAs: $10^{1.7}$ ng/g DM, $10^{1.5}$ ng/g DM; PFOS: $10^{2.0}$ ng/g DM, $10^{1.8}$ ng/g DM; total burden: $10^{2.2}$ ng/g DM, $10^{2.0}$ ng/g DM, respectively). Stable Isotope Analysis (SIA) indicated distinct foraging areas for UA, particularly in southern colonies with enriched δ13C values and δ15N enrichment, suggesting diverse food web structures influenced by Atlantic waters. In contrast, northern colonies showed uniformity in marine carbon intake and preference for less δ15N enriched sources. In addition, our findings suggest that PFAS exposure in these seabirds reflects chronic exposure to consistent dietary sources over time.

Despite limitations such as the absence of an isoscape around Iceland, our study underscores the vulnerability of Arctic seabirds to PFAS exposure and the persistence of these pollutants in Arctic ecosystems. The integration of SIA proves invaluable in deciphering foraging behavior and pollutant exposure. These findings contribute significantly to understanding pollution impact on Arctic wildlife, emphasizing the need for continued research in this domain.

Keywords: PFASs, Icelandic Seabirds, Stable Isotope Analysis, Foraging Ecology, Bioaccumulation, Pollution, Marine Ecosystems.

1   Introduction

Per- and polyfluoroalkyl substances (PFAS) are a group of synthetic chemicals that have been extensively used in various industrial and consumer products due to their oil- and water-repellent properties.[1] Their widespread use and environmental persistence have led to global dissemination, with PFASs being detected in various ecosystems, including marine environments.[2] Among the many organisms affected by PFASs contamination, seabirds have emerged as critical indicators due to their higher trophic level position and the propensity for bioaccumulation of these substances.

Seabirds, particularly species such as the common (Uria aalge, UA) and Brünnich's guillemots (Uria lomvia, UL), are integral to marine ecosystems and are considered sentinel species for monitoring environmental health.[3] These birds, residing predominantly in the North Atlantic, including regions around Iceland, are exposed to PFASs through their diet, which mainly consists of fish and other marine organisms. The bioaccumulative and potentially toxic nature of PFASs raises concerns regarding their impact on seabird health and, by extension, the broader marine ecosystem.
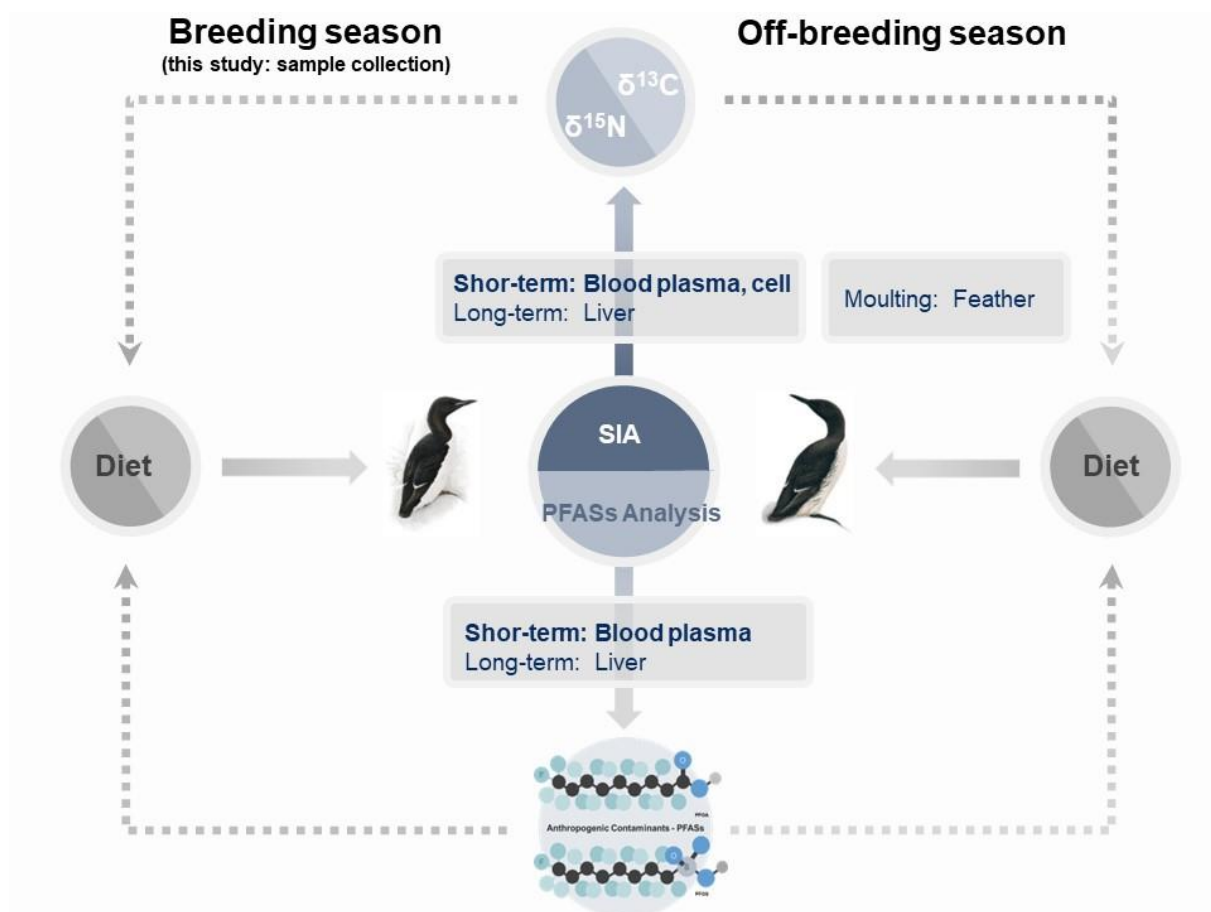

Figure 1. Concept Figure.

Understanding the temporal dynamics of PFAS exposure in seabirds is crucial for assessing ecological risks and impacts. This study focuses on dissecting these dynamics by employing a novel approach that integrates chemical analysis with stable isotope analysis. The use of stable isotopes, particularly nitrogen (δ15N), provides valuable insights into the foraging ecology of seabirds.[4] δ15N values in blood components, such as plasma and cells, serve as biomarkers for recent and medium-term dietary intake, respectively. This allows for the investigation of PFAS exposure over different timescales, providing a comprehensive understanding of the bioaccumulative patterns of these substances in seabirds.

The main objectives of this study are to identify the predominant PFAS compounds influencing Icelandic seabirds, to understand the temporal aspects of PFAS exposure, and to explore the potential of stable isotope analysis in elucidating the foraging ecology of these birds in relation to contaminant exposure. By achieving these objectives, we aim to contribute significantly to the fields of marine ecology and toxicology, offering essential insights for conservation efforts and policy formulation regarding PFAS management in marine environments.

2   Materials and Methods
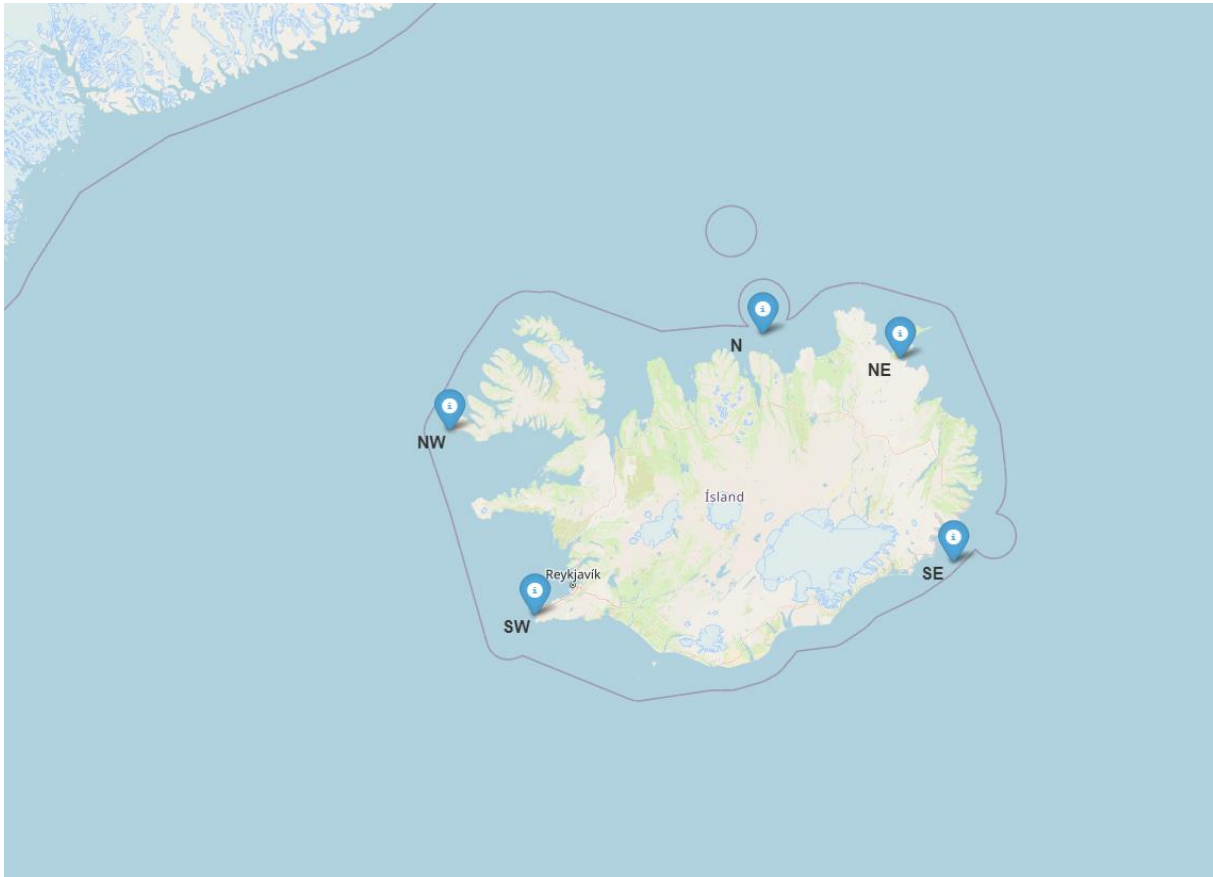
2.1   Study Area

Figure 2. Study Area

The fieldwork for this study, conducted in June 2018, involved sampling data from five unique guillemot colonies across Iceland, as depicted in Figure 2. These colonies are influenced by different ocean currents and climatic conditions. At Latrabjarg (65.50° N, 24.52° W) in the northwest, the colony is at the intersection of the warm Irminger Current and the cold East Greenland Current. Grimsey Island (66.57° N, 18.02° W), to Iceland's north, is predominantly under the influence of the Irminger Current, but also experiences the cooler East Icelandic Current. The Langanes peninsula (66.38° N, 14.54° W) in the northeast marks where the Irminger and East Icelandic Currents meet. Further along, Papey (64.59° N, 14.18° W), about 35 km northeast of the East Icelandic and North Atlantic Currents' convergence, adds another dimension to the study. Lastly, the Hafnaberg cliff (63.75° N, 22.75° W) in the southwest, situated in the North Atlantic Current, offers a contrasting environment. Detailed descriptions of oceanographic information were provided in previous studies.[5, 6]

The distribution and population dynamics of these seabirds have been detailed in previous studies.[7-10] At Latrabjarg, the largest colony, approximately 344,000 pairs of guillemots,

including a significant 34.3% of Black Guillemots, make their home. Grimsey Island, influenced by both the Irminger and East Icelandic Currents, supports 71,400 pairs, with 5.7% being Black Guillemots. The Langanes peninsula, a convergence point for major currents, is home to 46,800 pairs, including 6.2% Black Guillemots. In contrast, Papey and Hafnaberg, smaller colonies, house 3,700 and 419 pairs respectively, with Hafnaberg notable for its dwindling Black Guillemot population, which stood at about 5 pairs and was absent in 2019.

2.2 Sample Collection

The blood sampling methodology employed in this study follows established protocols as previously detailed in publications.[11, 12] Approximately 1 mL of blood was collected from each seabird via venipuncture. This technique was carefully executed to ensure minimal distress to the birds and maintain the integrity of the samples for subsequent analysis. Post collection, the blood samples underwent centrifugation using a Micro Star 12 centrifuge (VWR, Leuven, Belgium). This was carried out at a speed of 12,300 rpm for 4 minutes, effectively separating plasma and cells. The separated plasma and cells were then transferred into glass petri dishes. These samples were dried in a desiccator for a duration of 4 to 6 days. All blood samples were randomly collected in 2018, ensuring a representative cross-section of the seabird population at the selected breeding colonies. Blood sampling is non-lethal, allowing continued study of individuals after sampling.

2.3 PFASs Chemical Analysis

The PFASs analysis on plasma samples were performed at the Helmholtz-Zentrum Hereon in Geesthacht, Germany. The PFASs analytes are listed in Table X together with their chemical structures (SI).

The specific PFAS analytes under investigation are enumerated in Table x, alongside their respective chemical structures. A total of 16 PFAS compounds were analyzed, including 11 Perfluoroalkyl Carboxylic Acids (PFCAs) ranging from C4 to C14, 4 Perfluoroalkane Sulfonic Acids (PFSAs) (C4, C6, C8, and C10), and one Perfluoroether Carboxylic Acid (HFPO-DA).

Prior to extraction, individual blood plasma samples were spiked with ^13C-labelled PFAS standards to facilitate accurate quantification. The extraction and purification procedures were based on the methodology previous described[13], with further details provided in the Supporting Information. Subsequent to the purification process, the final extracts were carefully dried under a gentle stream of nitrogen and reconstituted in 250 µL of a specifically formulated injection standard solution.

The identification and quantification of PFASs were achieved through High-Performance Liquid Chromatography Tandem Mass Spectrometry (HPLC-MS/MS). The system comprised an HP1100 coupled with an API 4000 triple-quadrupole mass spectrometer, operating in multiple-

6

reaction monitoring (MRM) mode. This setup included an electrospray ionization (ESI) source, essential for the effective ionization of PFAS molecules.

A 10 µL aliquot of each sample was injected onto a C18 column (Synergi™ 4 µm, Fusion-RP 80 Å, LC Column 150 x 2 mm, Phenomenex). The separation was facilitated at a flow rate of 0.2 mL/min using a gradient mobile phase. This phase consisted of 95% water and 5% methanol with 5 mM ammonium acetate (solvent A) and 95% methanol with 5% water and 5 mM ammonium acetate (solvent B). The detailed mobile phase gradient profile is outlined in Table x.

The injection and instrumental conditions, along with the MS/MS parameters for target compounds, are described comprehensively in the Supporting Information. Quantification was anchored to a linear thirteen-point calibration curve, employing a 1/x weighting, ensuring high precision in PFAS measurement. For each batch of 10 samples, a blank was included to account for any potential background contamination. Concentrations were adjusted based on these blank values. The nominal detection limit was established at 0.1 ng/g dry weight, with the coefficients of determination (R² values) for each calibration curve being 0.990 or greater, reflecting the robustness of the analytical method.

2.4   Stable Isotope Analysis

Analysis of stable isotopes was performed at the Stable Isotope Facility of the Experimental Ecology Group, GEOMAR in Kiel, Germany.

Stable isotopes of nitrogen and carbon were determined using dried blood cell and plasma samples. Analysis was conducted on a xxx. Further details were described elsewhere (ambio, sci rep). The ratio of stable isotopes in parts per thousand (‰) are expressed as δ13C or δ15N, where

$$\delta = \left(\frac{Rsample}{Rreference} - 1\right) x\ 1000$$

Where R = 13C/12C or 15N/14N.

2.5   Statistical Treatments

In our study, comprehensive statistical analyses were meticulously conducted to interpret the complex dataset, primarily focusing on elucidating the relationships between PFAS concentrations in seabird plasma and their foraging behaviors as inferred from stable isotope ratios. These analyses were executed using Python.

Initially, data preparation steps included cleaning, normalization, and exploratory data analysis. Python's extensive libraries, such as Pandas and NumPy, facilitated efficient data manipulation

and preliminary statistical explorations. Descriptive statistics were generated to provide an initial understanding of the dataset's characteristics.

We employed PCA, a statistical technique used for dimensionality reduction while retaining most of the variability in the dataset, to identify underlying patterns in PFAS concentrations. This was achieved using Python's scikit-learn library, which offers a comprehensive suite of tools for machine learning and statistical modeling. The PCA allowed us to transform the complex PFAS data into principal components, simplifying the subsequent analysis.

To investigate the relationships between the identified PFAS patterns (principal components) and δ15N values in plasma and blood cells, linear regression models were developed. We utilized Python's statsmodels library to perform regression analysis, enabling us to quantify and interpret the association between our variables of interest. The choice of linear regression was based on preliminary analyses that suggested linear relationships.

Each regression model's statistical significance was assessed, with p-values being computed to determine the robustness of the associations observed. Model diagnostics, including checks for multicollinearity, homoscedasticity, and normality of residuals, were conducted to ensure the validity of our regression models.

For effective presentation and interpretation of results, data visualization played a pivotal role. We used Python's matplotlib and seaborn libraries for creating clear, informative plots, including scatter plots for visualizing relationships and histograms for distribution analysis. These visualizations aided in both the qualitative and quantitative understanding of our findings.

3   Results and Discussion

In this comprehensive assessment, we monitored 16 PFASS compounds, encompassing 11 perfluoroalkyl carboxylic acid (PFCA) homologues, 4 perfluoroalkyl sulfonic acid (PFSA) homologues, and 1 perfluoroalkyl ether carboxylic acid (PFECAs) homologue, across 112 blood plasma samples from 45 individuals of UL and 67 of UA. Descriptive statistics, including median concentrations, ranges, detection frequencies, and summed concentrations of homologue groups (e.g., Σ5PFCAs), are detailed in Table SI X.

Within the PFCAs, five long-chain homologues - PFNA, PFDA, PFUnDA, PFDoDA, and PFTrDA (C9 - 13) - were consistently detected in all samples from both UL and UA. PFTeA exhibited a notable detection rate of 86% across both species, with a higher prevalence in UA (93%) compared to UL (76%). The presence of PFOA was relatively uniform between the two species, detected at rates of 62% in UL and 63% in UA. Conversely, PFHpA was rarely observed, present in only 4% of UL samples and undetectable in UA. Short-chain PFCAs - PFBA, PFPeA, and PFHxA - were not detected in any samples.

Among the PFSAs, ∑PFOS (encompassing linear and branched isomers) was identified in all samples, indicating its ubiquitous presence. PFDS was observed in approximately half of the individuals from both species (56% in UL and 49% in UA). PFHxS was detected less frequently, appearing in 34% of UA and only 18% of UL. PFBS was not detected in either species. Additionally, HFPO-DA - a PFECAs homologue - was not quantitatively present in the samples.

Our study primarily examined C9 – 13 PFCAs and ΣPFOS, which were universally detected, to facilitate a targeted and statistically robust analysis of PFASs exposure in Icelandic seabirds.

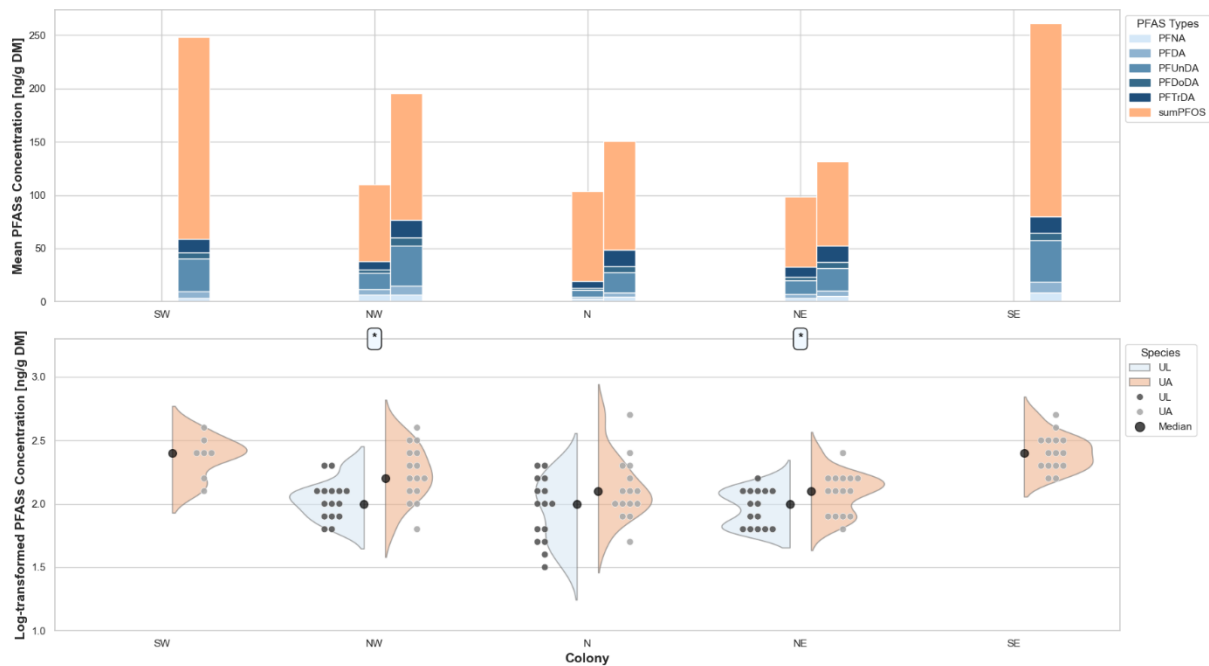## 3.1   Descriptive Analysis of PFASs Analysis

Figure 3. Descriptive Demographic Analysis of PFASs Concentrations in UA & UL Across Five Colonies. This figure represents the median concentrations of various PFASs compounds (PFNA, PFDA, PFUnDA, PFDoDA, PFTriDA, and ∑PFOS) across five colonies (SW, NW, N, NE, SE) depicted in the bar plots, alongside the distribution and range of the total burden (∑6PFASs) within the two seabird species illustrated in the split violin plots with swarm overlay.

Our study assesses the concentrations of PFASs in the plasma of Icelandic seabirds, focusing on long-chain PFCAs and ∑PFOS across multiple colonies. The median concentrations of ∑PFOS were found to be predominant in the PFASs profile for both UA and UL. UA demonstrated a ∑PFOS range of 69.7 to 162.0 ng/g DM, comprising 62 - 73% of the total PFASs burden. In contrast, UL exhibited a lower ∑PFOS range of 60.6 to 72.4 ng/g DM, accounting for 70 - 89% of their total PFASs burden. Notably, at colony N, UL showed an elevated proportion of ∑PFOS, reaching 89% of their total PFASs burden despite having the second-lowest concentration at 61.8 ng/g DM. This pattern suggests a pervasive ecological presence or bioaccumulative potential of ∑PFOS in the marine ecosystem, consistent across species.[14-16]

Concomitant to ∑PFOS, PFUnDA was observed in elevated concentrations for both species. UA displayed PFUnDA concentrations ranging from 14.7 to 32.8 ng/g DM, contributing 12 to 19% to the total burden. UL showed approximately half the concentration of UA within the same colonies, with values spanning from 5.8 to 13.9 ng/g DM and accounting for 4 to 12% of the total burden. Despite being the second most abundant compound, PFUnDA's proportion relative to ∑PFOS remains low.

10

PFTrDA also presented with considerable median concentrations following PFUnDA in both species - ranging from 10.8 to 16.1 ng/g DM in UA and 4.1 to 9.9 ng/g DM in UL. However, its contribution to the total PFASs burden fell below 10%. The occurrence of other long-chain PFCAs, such as PFNA, was comparable and low in abundance for both species, aligning with patterns reported in previous research.[17-22]

The aggregate total burden of PFASs (∑6PFASs) was log-transformed to reflect exposure levels. This transformation elucidates the variability and distribution of total burden among the seabird species across the colonies.

A wide range of PFASs levels was evident for both species, UL and UA, indicative of individual variability within each population. Despite this interindividual variability, the median total burden showed a degree of interspecies consistency, with UL maintaining a median level burden of approximately 2.0, whereas UA ranged from 2.1 to 2.4. Within the northern sectors, UA values varied from 2.1 to 2.2, while the southern sectors registered higher at 2.4.

An anomaly was observed in the distribution pattern of UL at the NE colony, which deviated from normality, suggesting a possible bimodal distribution, whereas other colonies' total burden levels conformed to a normal distribution.

3.2   Principal Component Analysis (PCA) Discerned Bioaccumulative Pattern

In this study, Principal Component Analysis (PCA) was employed to manage the inherent complexity of our extensive PFASs dataset. Through PCA, we achieved a significant reduction in dimensionality, transforming the observed variables into a series of linearly uncorrelated principal components (PCs). Our analysis predominantly focused on the PCs accounting for the highest variance, aiming to elucidate the clustering of PFASs and examine the influence of their specific properties on biological behavior. This methodology is anticipated to illuminate the complex interactions and dynamics of PFASs, thereby enhancing our understanding of their bioaccumulative impact.

The analysis through PCA is shedding new light on the characteristics and behaviors of PFAS compounds. The first three PCs - PC1, PC2, and PC3 - cumulatively account for over 95% of the total variance, with PC1 alone representing 79 %. This significant proportion suggests that these components capture the primary trends and variances within the dataset.

PC1, characterized by the highest variance, predominantly reflects a variance across a broad spectrum of the long-chain PFCAs homologues. This is evidenced by negative loadings in the range of -0.40 to -0.45 from C9-13 PFCAs, contrasting with a slightly lower contribution of -0.25 from ∑PFOS. Higher scores on PC1 likely indicate lower levels of individual C9-13 PFCAs relative to ∑PFOS. The similar magnitude of loadings for C9-13 PFCAs suggests that PC1

may represent a balance between the presence of C9-13 PFCAs and ∑PFOS levels within the samples, possibly hinting at a shared source or influence affecting these compounds.

PC2, in contrast, is defined by a strong positive loading from ∑PFOS (0.95), with negligible contributions from the C9-13 PFCAs. This distinct variance captured by PC2 points to its specificity in differentiating samples based on variations in ∑PFOS levels, independent of C9-13 PFCAs levels.

PC3 shows a predominant positive loading from PFNA (0.81), with other PFASs contributing minimally. The prominence of PFNA in PC3 implies a unique variability in its levels compared to other compounds, suggesting a distinct behavior or distribution pattern for PFNA within the dataset. However, given its marginal variance contribution (5%), we primarily focus our analysis on PC1 and PC2, which collectively explain approximately 92 % of the total variance. This approach underscores our commitment to a simplified and clear analysis.

In summary, PCA effectively differentiates PFASs based on their functional groups, as demonstrated in the mappings on the first two principal components (PC1 and PC2). This segregation not only underscores the chemical diversity within PFASs, but also reveals specific bioaccumulative patterns. For instance, PC1 primarily represents a broad spectrum of long-chain PFCAs homologues, which correspond to variations in overall exposure levels. Conversely, PC2 provides a focused analysis of ∑PFOS, underscoring its unique behavior. Intriguingly, the bioaccumulative patterns revealed by PCA show remarkable consistency with existing toxicological findings, linking molecular characteristics to biological behavior and impact.

This observation becomes more evident when examining the molecular interactions of PFASs. Predominantly, PFASs bind to albumin[23, 24], a prevalent protein in blood plasma in vertebrates[25], while also showing affinity to other proteins, such as lipoproteins.[26] This binding affinity is significantly influenced by both the chain length and the functional group of the PFASs molecule.[2, 27] Typically, PFASs with longer chains (exceeding seven carbon atoms)[28] demonstrate a stronger propensity for protein binding. Notably, PFSAs with sulfonate groups exhibit a more robust binding affinity to proteins compared to PFCAs with carboxylate groups. This stronger affinity for biological tissues, coupled with a heightened resistance to metabolic breakdown, culminates in a more pronounced biomagnification effect within the food chain.[29, 30]

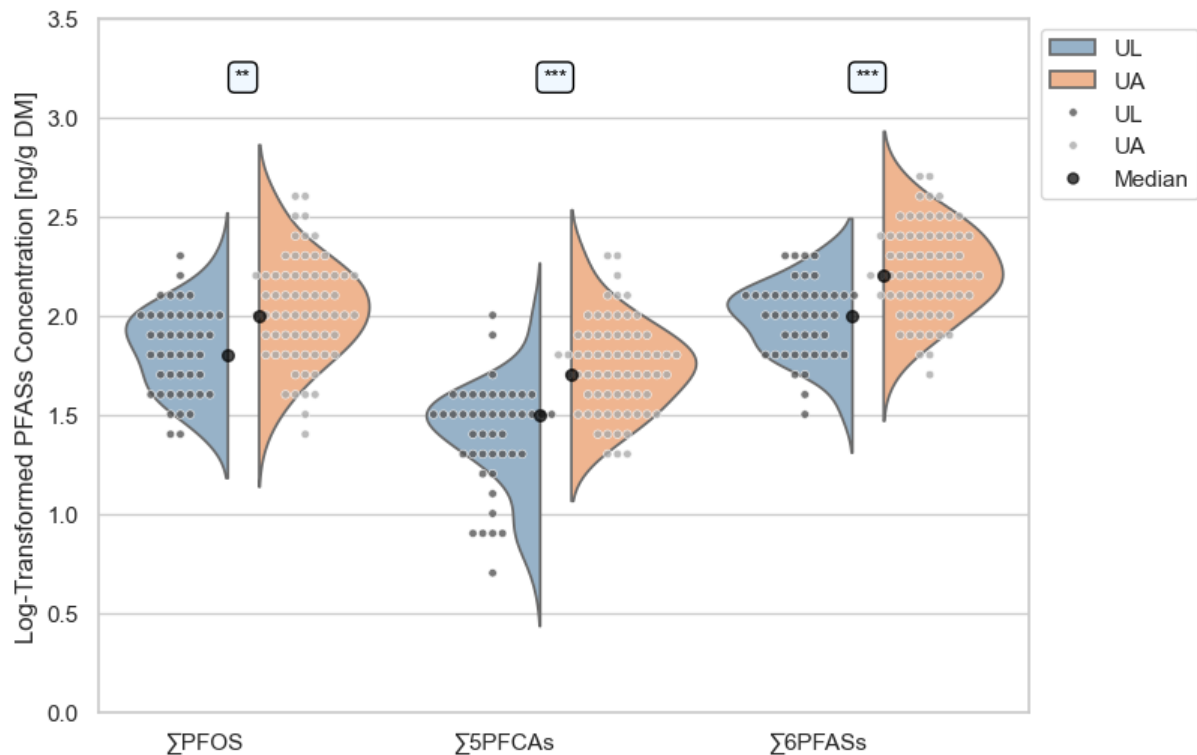## 3.3   Interspecies Comparison on Bioaccumulative Patterns

Figure 4. Interspecies Comparison.

In this segment of our study, we leveraged the insights gained from PCA to investigate interspecies differences in relation to the observed bioaccumulative patterns. Our analysis centered on ∑5PFCAs and ∑PFOS, corresponding to PC1 and PC2 respectively, alongside an assessment of the total burden as reflected by ∑6PFASs. We observed that the distribution of ∑5PFCAs in UA conformed to a normal distribution, whereas UL exhibited a distinctly non-normal distribution. This variance necessitated the use of the non-parametric Mann-Whitney U-test for comparing median levels across the species.

Our statistical examination revealed pronounced differences in PFASs profiles between the species. Notably, ∑PFOS levels in UL were lower (median: 1.8) and exhibited a narrow distribution, indicative of a consistent exposure pattern among individuals. In contrast, UA showed higher median ∑PFOS levels (median: 2.0) with greater dispersion, suggesting a more varied pattern of accumulation and significant divergence ($p < 0.01$).

The pattern for ∑5PFCAs differed; UL showed a skewed distribution with lower levels (median: 1.5), while UA displayed a more symmetric distribution with higher median levels (median: 1.7, $p < 0.001$). This suggests a uniform and elevated exposure in UA. These disparities in PFAS profiles are indicative of potential differences in bioaccumulative capacities or exposure sources between the species, raising ecological concerns regarding the impacts of PFASs accumulation.

The analysis of ∑6PFASs further highlighted the heightened PFAS burden in UA (median: 2.2) compared to UL (median: 2.0). This was statistically significant ($p < 0.001$) and aligned with the observed patterns in the other metrics, suggesting a consistent trend across various PFASs measures. This finding warrants further exploration into the ecological and biological factors driving PFASs distribution and bioaccumulation in these species.

These interspecies discrepancies could potentially be attributed to variations in diet, habitat utilization, and migratory behaviors, which are pivotal in determining environmental exposure and bioaccumulation potential of PFASs. The ecological implications of these findings are substantial, as they may influence the health and survival of these seabird species, with possible broader effects on the structure and function of marine ecosystems.

3.4   Spatial Comparison on Bioaccumulative Patterns

To understand the distribution of PFASs across seabird colonies, we first conducted statistical validation of data distributions. For UA, data adhered to the criteria for normality and homogeneity of variance, thus validating the use of parametric statistical methods. In contrast, UL exhibited non-normal distributions and heterogeneous variances, necessitating the employment of non-parametric approaches. These initial analyses suggest species-specific distribution patterns of PFASs, potentially driven by differing environmental conditions or inherent species characteristics.

A one-way ANOVA conducted for UA revealed significant heterogeneity in ∑PFOS and ∑6PFASs across colonies (∑PFOS: $F = 8.31$, $p < 0.0001$; ∑6PFASs: $F = 7.62$, $p < 0.0001$), indicating notable bioaccumulation variations. Conversely, ∑5PFCAs showed a more uniform distribution ($F = 2.35$, $p = 0.06$), pointing to a consistent bioaccumulation pattern for this group of compounds.

Further analysis using Tukey's HSD test identified significant differences in mean PFASs levels among UA colonies. Notably, southern colonies (SE and SW) consistently exhibited higher ∑PFOS and ∑6PFASs levels compared to northern colonies (N and NE). This pattern suggests geographical influences on PFASs bioavailability, possibly related to local dietary sources or distinct ecological behaviors affecting exposure levels.

The total PFASs burden in UA, indicated by ∑6PFASs, appears predominantly influenced by ∑PFOS levels. This aligns with the known persistence and bioaccumulative properties of ∑PFOS, contributing to a stable overall PFAS load across colonies, despite variations in other PFAS subgroups.

For UL, significant spatial variation was observed only for ∑5PFCAs ($H = 10.03$, $p < 0.01$), with notable differences in median levels between N and NE colonies (p-corrected < 0.05). However, the uniformity in ∑PFOS levels ($p = 0.72$) across colonies suggests a consistent

bioaccumulation pattern. Similarly, ∑6PFASs showed no significant spatial differences (p = 0.65), indicating a consistent total load despite the variability in ∑5PFCAs. This pattern might be largely attributed to the proportion of ∑PFOS within the total PFASs measure.

The geographic disparities in PFASs distribution for UA, characterized by pronounced differences between northern and southern colonies, contrast with the more uniform distribution in UL colonies from similar latitudes. These observations may reflect localized environmental factors or the influence of the colonies' latitudinal range on PFASs bioavailability.

The marine currents surrounding Iceland, specifically the warm Atlantic waters in the south and the cold Arctic Overflow in the north, are critical in mediating PFASs bioavailability within the marine ecosystem. The southern region, closer to anthropogenic PFASs sources, bears a higher pollution load. The mobility and persistence of PFASs, alongside their physicochemical properties, determine their dispersion and concentration levels in these marine environments.

Differences in seabird foraging strategies, adapted to the unique conditions of the two currents, further influence PFASs exposure and accumulation. The diverse prey base in the warmer Atlantic waters may increase bioaccumulation potential in seabirds, whereas the simpler food web in the colder Arctic waters could provide some level of protection against these contaminants.

3.5   Stable Isotope Analysis
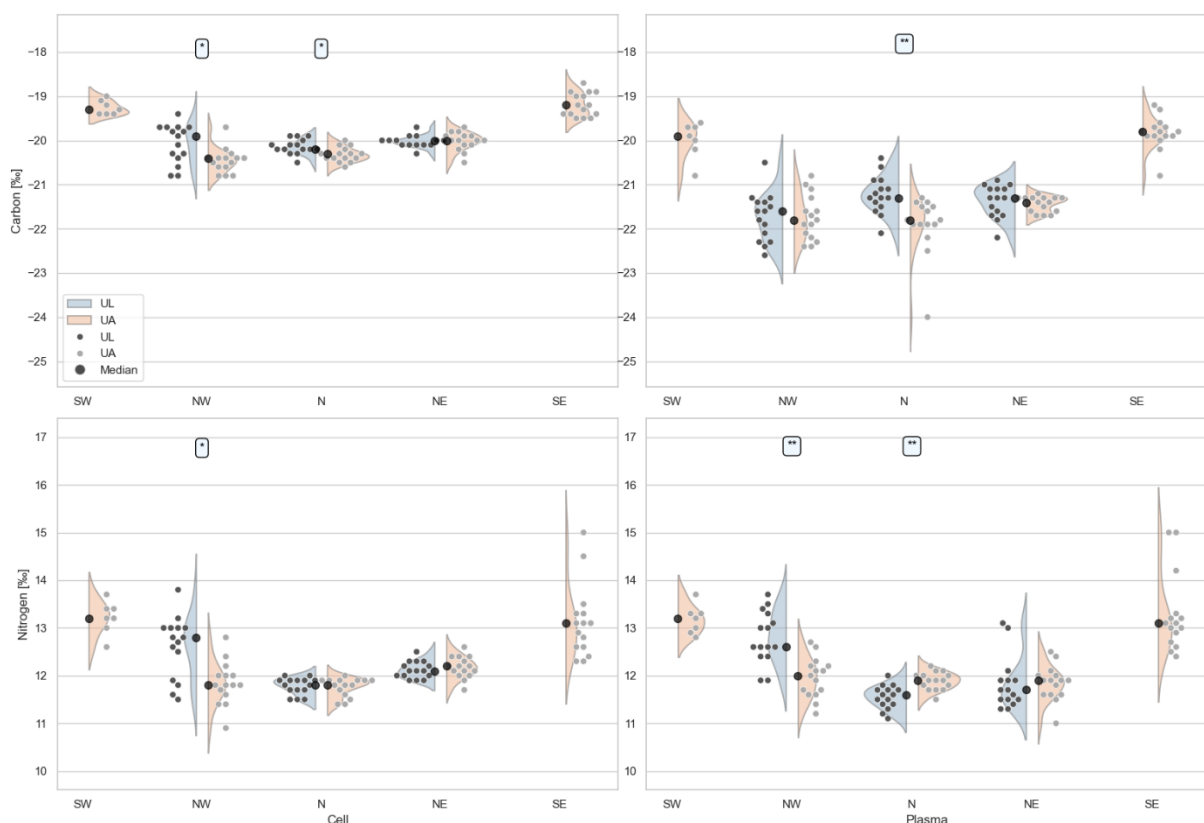
We investigate the stable isotopes of carbon (δ13C) and nitrogen (δ15N) in both cellular and plasma fractions of UA and UL. The analysis of stable isotopes serves as a pivotal tool in understanding the dietary patterns and ecological interactions of these birds. Due to inherent differences in the turnover rates of cells and plasma, these isotopic measurements offer distinct temporal insights into the seabirds' foraging behaviors.

Plasma, being a rapidly metabolizing component, reflects recent dietary intake. The turnover rate of plasma in seabirds, as evidenced in related avian studies, typically ranges from a few days to about a week.[31] This rapid turnover implies that the isotopic composition of plasma primarily indicates dietary inputs from the preceding days, offering a near real-time snapshot of the seabirds' recent foraging activities.

In contrast, cellular components have a significantly slower turnover rate, generally spanning several weeks.[31] For seabirds, the cellular isotopic signatures are indicative of dietary inputs over an extended period, typically reflecting the accumulated dietary history over the past three to four weeks. This slower integration of isotopic signals in cellular components provides a broader, more integrated view of the seabirds' foraging strategies and dietary preferences over a longer timescale.

Previous investigations into the foraging ecology of UA and UL have provided foundational insights into their foraging behaviors through the analysis of stable isotopes in cellular tissues.[11] Published findings have elucidated their dietary patterns prior to the breeding season and ecological niches of these species, revealing distinct latitudinal patterns emerged. These patterns reveal nuanced differences in dietary intake and foraging strategies across the northern and southern sectors of their respective ranges.

Isotopic measurements of $\delta^{13}C_{cell}$ and $\delta^{15}N_{cell}$ in UA and UL suggest both species exploit similar carbon sources within their marine environments, with UA ranging from -20.3‰ to -19.2‰ and UL from -20.2‰ to -19.9‰. Despite these overlaps, a notable expansion in the isotopic dynamic range was observed at the NW colony for both species, with ranges of 1.1‰ and 1.4‰, respectively. This isotopic breadth indicates a more varied diet or diverse foraging zones, contrasting with colonies where a more constricted isotopic range was recorded.

Median $\delta^{13}C_{cell}$ values for UA and UL at colony N converge, yet the dynamic ranges are relatively limited. Mann-Whitney U test outcomes reveal a statistically significant divergence in foraging behaviors between the two species. UL demonstrate an isotopic inclination towards more enriched $\delta^{13}C$ values, denoting a potential preference for foraging regions with a higher baseline carbon isotopic signature. Inversely, UA species manifest a tendency towards more negative δ13C values, potentially indicating exclusive foraging grounds or distinctive prey species selection, despite their proximity to UL foraging territories. At the NE colony, the $\delta^{13}C_{cell}$

values exhibit minimal variability, which could signify a specialized foraging behavior or a marine carbon pool with reduced variability within this locale.

The broader dynamic range in $\delta^{13}C_{cell}$ associates with an increased range in $\delta^{15}N_{cell}$ values, suggesting that a varied carbon intake is linked to a more extensive array of nitrogen sources. This isotopic pattern may reflect a wider trophic diversity or opportunistic feeding across multiple food web levels. Conversely, a narrower $\delta13C$ range is associated with a more limited $\delta15N$ range, suggesting a more specialized or consistent dietary regime, both in terms of carbon and nitrogen intake.

In contrast, in the southern sectors, despite the dynamic range in $\delta^{13}C_{cell}$ being narrower, indicating less variability in carbon sources, the $\delta^{15}N_{cell}$ range is observed to be wider. This wider range in $\delta15N$ could suggest that, although the carbon intake is relatively consistent, there is a greater diversity in the trophic levels of prey being consumed. It may also reflect seasonal or interannual variations in prey availability, potentially driven by different oceanographic conditions or ecological processes specific to the southern habitats.

The plasma isotopic composition provides insights into the recent dietary sources of carbon and nitrogen. For UL, the median $\delta13C$plasma values range narrowly from -21.6 ‰ to -21.3 ‰, suggesting a relatively consistent marine carbon source. However, an observable variation (> 1 ‰) in dynamic range suggests dietary diversity. Like the cellular analysis, a notable isotopic expansion was observed for UL at NW, with a dynamic range extending to 2.1‰, the broadest among their colonies. This isotopic range diminishes progressively from west to east, culminating in a reduced variance of 1.3‰ at NE. The H-test indicates a lack of significant isotopic variation among colonies, suggesting a degree of homogeneity in carbon sources across the geographical range.

For, $\delta13C$plasma values exhibit a broader oscillation between -21.8 ‰ and -19.8 ‰. While most colonies display a dynamic range exceeding 1 ‰, the NE colony presents a conspicuously narrow range of 0.5 ‰. This pattern is further substantiated by the H-test and posthoc analyses, which reveal consistent and significant isotopic variances between northern and southern sectors. The northern sector median values converge between -21.8‰ to -21.4‰, contrasting with the southern sector, where median $\delta13C$plasma values are notably more enriched, reaching -19.8‰ at SE and -19.9‰ at SW.

Analysis of $\delta15N$plasma values in UL revealed median values oscillating from 11.6 ‰ to 12.6 ‰, indicating access to a relatively wide array of marine nitrogen sources. The dynamic range of $\delta15N$plasma was most pronounced at the NW and NE colonies, reaching up to 1.8‰, which suggests a substantial variability in the nitrogen-based diet or a broader niche within the marine trophic structure. In contrast, the N colony exhibited a more homogeneous $\delta15N$plasma signature at 0.9 ‰, indicative of a more consistent dietary intake among individuals.

In UA, δ15Nplasma values varied from 11.9‰ to 13.2‰, aligning with the diverse carbon sources previously described. Statistical tests substantiated a distinct variation in δ15N values between northern and southern sectors. In northern colonies, median δ15Nplasma values ranged narrowly from 11.9‰ to 12.0‰, with NW and NE again demonstrating a wider dynamic range of 1.5 ‰, in stark contrast to the narrower range of 0.7 ‰ observed at N. Conversely, in the southern sector, δ15Nplasma values were notably higher at SE (13.1 ‰) with an extensive dynamic range of 2.6 ‰, and similarly elevated at SW (13.2‰), albeit with a more constrained range of 0.9 ‰.

A significant isotopic discrepancy in plasma δ13C and δ15N values was discerned between UA and UL at N. The Mann-Whitney U tests revealed distinct differences (δ13C: U = 31.0, p < 0.001; δ15N: U = 194.0, p < 0.001), with UL demonstrating more enriched δ13C values. This enrichment in δ^13C suggests that UL at N may be foraging within marine areas characterized by a different baseline carbon isotopic composition, or they may have dietary preferences that favor carbon sources with a more positive isotopic value.

Further differentiation in δ15Nplasma values was observed, with UL exhibiting higher values than UA at NW, indicative of 1 δ5N enriched diet. Conversely, at N, UL showed significantly lower δ15Nplasma values than UA. This divergence in nitrogen isotopic values may reflect varied dietary interactions, with UL at N potentially feeding on prey with depleted δ15N levels.

The δ13C and δ15N isotopic profiles provide insightful revelations into the foraging behaviors and dietary preferences of UL and UA. Isotopic data delineate spatial variations that are emblematic of the distinct ecological dynamics within seabird colonies situated around the Icelandic marine environment.

In the northern sectors, the aggregation of median δ13C values signifies a uniformity in marine carbon intake, potentially reflecting the influence of the cooler, less saline Arctic waters that converge in these regions. The isotopic homogeneity might be attributable to the consistency in carbon sources available within the Arctic-influenced waters, which affect the primary productivity and, consequently, the marine food web exploited by the seabirds.

Contrastingly, in the southern sectors, the enriched δ13C values are indicative of foraging niches that may be influenced by the warmer, more saline currents of the North Atlantic. The shift towards a heavier carbon isotopic composition could be a consequence of the seabirds' dietary response to the different oceanic conditions, which affect the distribution and composition of prey species.

The observed δ15N isotopic variability across the colonies underscores the seabirds' dietary plasticity, capable of reflecting short-term and medium-term changes in trophic interactions. The expansive dynamic ranges in certain colonies, particularly where oceanic currents

intersect, may signify an opportunistic dietary adaptation to the convergence zones of diverse marine currents, leading to a variable diet.

The pronounced δ15N enrichment in southern colonies suggests a (trophic) shift towards δ15N enriched prey, which may be more abundant or accessible due to the interplay between the North Atlantic Current and the coastal waters around Iceland. Such an elevation could be indicative of a diversified food web structure in these southern marine environments, shaped by the influx of nutrient-rich Atlantic waters.

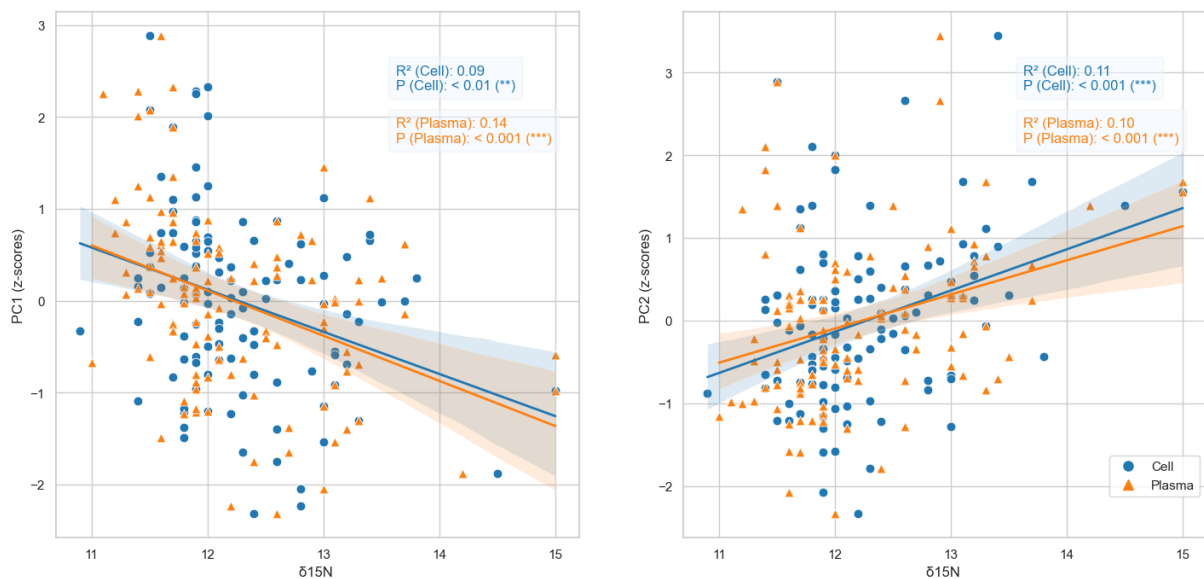## 3.6 Temporal Dynamics of Bioaccumulation

Figure 5. Temporal Dynamics

To explore the temporal dynamics of PFASs exposure in Icelandic seabirds, our study employed simple linear regression to investigate the association between z-scores derived from principal component (PC) loadings, representing standardized PFASs exposure, and δ15N values in blood components. These components encompass blood cells, indicative of medium-term uptake, and plasma, reflective of recent dietary uptake. The findings are illustrated in Figure 5.

Our linear regression analysis, correlating PC1 (characterizing C9-13 PFCAs profiles) with δ15N values in blood cells and plasma, yielded low R^2 values of 0.09 and 0.14, respectively. This indicates limited explanatory power of C9-13 PFCAs profiles in accounting for variations in δ15N values across both sample types. Additionally, the regression involving PC2 (encompassing ∑PFOS profiles) and δ15N values exhibited similarly low R^2 values of 0.11 in cells and 0.10 in plasma, further indicating a weak relationship with δ15N variations. The overlapping confidence intervals (CI) observed in these analyses implies that the

bioaccumulative pattern, as reflected by the PCs, do not significantly differ over the time frames denoted by the δ15N values in plasma and blood cells.

Despite these low R^2 values, the statistical significance of these associations is reinforced by p-values less than 0.01. While the observed associations are weak, they are not attributable to random data variations. This outcome suggests a level of association between δ15N values and the bioaccumulative patterns of PFASs, though not a robust one.

The limited recent dietary absorption may suggest low bioavailability of PFASs near seabird breeding colonies. Our findings indicate that the bioaccumulative patterns, as denoted by PC1 and PC2, are not primarily derived from recent dietary intake, whether on a short-term (within a week) or medium-term (within a month) basis. Instead, these patterns appear to reflect chronic exposure to dietary sources that remain relatively constant over these time frames. The persistent nature of these bioaccumulative patterns tends to obscure their correlation with recent or medium-term dietary sources. As a result, the PFASs levels observed likely represent an accumulation from previous seasons, potentially indicative of higher exposure in wintering habitats.

It's important to note that the half-life of PFASs, particularly in avian tissues, remains significantly understudied. This gap in knowledge becomes evident when considering the variability in PFASs elimination across different species. For instance, in mallard (Anas platyrhynchos) serum, the half-life of PFOS is approximately 13.6 days, and in northern bobwhite quails (Colinus virginianus) serum, it's around 20.1 days.[32] This duration increases substantially in male chickens (Gallus gallus)[33], where the half-life reaches up to 125 days. In male rats, the half-life exceeds 89 days[32], and in cynomolgus monkeys (Macaca fascicularis) serum, it ranges between 100 and 200 days[34]. Humans, however, exhibit a significantly longer elimination half-life of PFOS, averaging about 8.6 years.[35] Recognizing this variance, and the notable lack of detailed studies on PFAS half-life in avian species, underscores the need for comprehensive research in this area. Establishing reliable estimates for the elimination half-life of PFASs in an organism's tissue, particularly in birds, is crucial. Such data will allow for a more standardized and accurate assessment of PFAS persistence and exposure over time within various organisms.

4   Synthesis of Findings

This study not only delves into the temporal dynamics of per- and polyfluoroalkyl substances (PFASs) exposure in Icelandic seabirds but also innovates by applying stable isotope analysis to understand their foraging ecology. By combining principal component analysis (PCA) with linear regression, and integrating stable isotope analysis, we provide a nuanced perspective on the bioaccumulative patterns of PFAS and their potential dietary sources.

PCA identified two principal components, PC1 and PC2, encapsulating the bioaccumulative patterns of PFASs in the seabirds. PC1 correlated with long-chain C9-13 PFCAs homologues, while PC2 was primarily associated with ΣPFOS, setting the foundation for understanding PFAS impact on seabirds.

Employing stable isotopes of carbon (δ13C) and nitrogen (δ15N) from cellular and plasma fractions of seabird blood, we gleaned essential insights into their foraging behavior. Plasma δ15N values, reflective of recent diet, and cellular δ15N values, indicative of medium-term dietary trends, were pivotal in elucidating the temporal aspects of PFAS exposure. This innovative application of stable isotopes forges new ground in linking foraging ecology with contaminant dynamics.

Our linear regression analysis, correlating PC1 and PC2 with δ15N values, revealed low R^2 values, indicating a limited impact of these PFAS profiles on δ15N variations. However, the statistically significant p-values (< 0.01) suggest a discernible, though weak, relationship between δ15N values and PFAS bioaccumulative patterns.

The results point to a relatively low bioavailability of PFAS around the seabirds' breeding colonies. The chronic nature of exposure, inferred from bioaccumulative patterns not primarily deriving from recent dietary sources, emerges as a crucial insight. This pattern suggests that the observed PFAS levels may accumulate over extended periods, potentially reflecting exposure at wintering grounds.

The integration of stable isotope analysis in this study marks a significant advancement in our understanding of foraging ecology in the context of exposure. It highlights the value of stable isotopes as a tool in ecological research, particularly for tracing the origins of environmental contaminants in marine ecosystems. This methodology enhances our understanding of the linkage between dietary sources and pollutant accumulation, which is imperative for marine ecology, toxicology, and conservation policy.

Our research underscores the complexity of PFASs contamination and the necessity of considering temporal dynamics and foraging behavior in environmental exposure assessments. The associations revealed between PFAS patterns and δ15N values offer novel insights into

the protracted nature of PFAS bioaccumulation in Icelandic seabirds, enriching our comprehension of their exposure pathways and potential ecological impacts.

5   Reference

(1) OECD. Toward a new comprehensive global database of per- and polyfluoroalkyl substances (PFASs): Summary report on updating the OECD 2007 list of per and polyfluoroalkyl substances (PFASs). 39 ed.; Development, O. f. E. C.-o. a., Ed.; Paris, France, 2018.

(2) Kelly, B. C.; Ikonomou, M. G.; Blair, J. D.; Surridge, B.; Hoover, D.; Grace, R.; Gobas, F. A. P. C. Perfluoroalkyl Contaminants in an Arctic Marine Food Web: Trophic Magnification and Wildlife Exposure. *Environ. Sci. Technol.* **2009**, *43* (11), 4037-4043. DOI: 10.1021/es9003894.

(3) Furness, R. W.; Camphuysen, K. Seabirds as monitors of the marine environment. *ICES Mar. Sci. Symp.* **1997**, *54* (4), 726-737. DOI: 10.1006/jmsc.1997.0243 (acccessed 3/10/2022).

(4) Gannes, L. Z.; O'Brien, D. M.; del Rio, C. M. STABLE ISOTOPES IN ANIMAL ECOLOGY: ASSUMPTIONS, CAVEATS, AND A CALL FOR MORE LABORATORY EXPERIMENTS. *Ecology* **1997**, *78* (4), 1271-1276. DOI: https://doi.org/10.1890/0012-9658(1997)078[1271:SIIAEA]2.0.CO;2.

(5) Casanova-Masjoan, M.; Pérez-Hernández, M. D.; Pickart, R. S.; Valdimarsson, H.; Ólafsdóttir, S. R.; Macrander, A.; Grisolía-Santos, D.; Torres, D. J.; Jónsson, S.; Våge, K.; et al. Along-Stream, Seasonal, and Interannual Variability of the North Icelandic Irminger Current and East Icelandic Current Around Iceland. *Journal of Geophysical Research: Oceans* **2020**, *125* (9), e2020JC016283. DOI: https://doi.org/10.1029/2020JC016283.

(6) Huang, J.; Pickart, R. S.; Huang, R. X.; Lin, P.; Brakstad, A.; Xu, F. Sources and upstream pathways of the densest overflow water in the Nordic Seas. *Nature Communications* **2020**, *11* (1), 5389. DOI: 10.1038/s41467-020-19050-y.

(7) Garðarsson, A.; Guðmundsson, G.; Lilliendahl, K. The numbers of large auks on the cliffs of Iceland in 2006–2008. *Bliki* **2019**, *33*, 35-46.

(8) Frederiksen, M.; Descamps, S.; Erikstad, K. E.; Gaston, A. J.; Gilchrist, H. G.; Grémillet, D.; Johansen, K. L.; Kolbeinsson, Y.; Linnebjerg, J. F.; Mallory, M. L.; et al. Migration and wintering of a declining seabird, the thick-billed murre Uria lomvia, on an ocean basin scale: Conservation implications. *Biological Conservation* **2016**, *200*, 26-35. DOI: https://doi.org/10.1016/j.biocon.2016.05.011.

(9) Linnebjerg, J. F.; Frederiksen, M.; Kolbeinsson, Y.; Snaethórsson, A. Ö.; Thórisson, B.; Thórarinsson, T. L. Non-breeding areas of three sympatric auk species breeding in three Icelandic colonies. *Polar Biology* **2018**, *41* (10), 1951-1961. DOI: 10.1007/s00300-018-2334-1.

(10) Frederiksen, M.; Descamps, S.; Elliott, K. H.; Gaston, A. J.; Huffeldt, N. P.; Kolbeinsson, Y.; Linnebjerg, J. F.; Lorentzen, E.; Merkel, F. R.; Strøm, H.; et al. Spatial variation in vital rates and population growth of thick-billed murres in the Atlantic Arctic. *Marine Ecology Progress Series* **2021**, *672*, 1-13.

(11) Bonnet-Lebrun, A.-S.; Larsen, T.; Thórarinsson, T. L.; Kolbeinsson, Y.; Frederiksen, M.; Morley, T. I.; Fox, D.; Boutet, A.; le Bouard, F.; Deville, T.; et al. Cold comfort: Arctic seabirds find refugia from climate change and potential competition in marginal ice zones and fjords. *Ambio* **2021**. DOI: 10.1007/s13280-021-01650-7.

(12) Bonnet-Lebrun, A.-S.; Larsen, T.; Frederiksen, M.; Fox, D.; le Bouard, F.; Boutet, A.; Þórarinsson, Þ. L.; Kolbeinsson, Y.; Deville, T.; Ratcliffe, N. Effects of competitive pressure and habitat heterogeneity on niche partitioning between Arctic and boreal congeners. *Scientific Reports* **2021**, *11* (1), 22133. DOI: 10.1038/s41598-021-01506-w.

(13) Kannan, K.; Koistinen, J.; Beckmen, K.; Evans, T.; Gorzelany, J. F.; Hansen, K. J.; Jones, P. D.; Helle, E.; Nyman, M.; Giesy, J. P. Accumulation of Perfluorooctane Sulfonate in Marine Mammals. *Environmental Science & Technology* **2001**, *35* (8), 1593-1598. DOI: 10.1021/es001873w.

(14) Butt, C. M.; Berger, U.; Bossi, R.; Tomy, G. T. Levels and trends of poly- and perfluorinated compounds in the arctic environment. *Science of the Total Environment* **2010**, *408* (15), 2936-2965. DOI: 10.1016/j.scitotenv.2010.03.015.

(15) Hedgespeth, M. L.; Taylor, D. L.; Balint, S.; Schwartz, M.; Cantwell, M. G. Ecological characteristics impact PFAS concentrations in a U.S. North Atlantic food web. *Sci Total Environ* **2023**, *880*, 163302. DOI: 10.1016/j.scitotenv.2023.163302 From NLM Medline.

(16) Munoz, G.; Mercier, L.; Duy, S. V.; Liu, J.; Sauvé, S.; Houde, M. Bioaccumulation and trophic magnification of emerging and legacy per- and polyfluoroalkyl substances (PFAS) in a St. Lawrence River food web. *Environmental Pollution* **2022**, *309*, 119739. DOI: https://doi.org/10.1016/j.envpol.2022.119739.

(17) Butt, C. M.; Mabury, S. A.; Muir, D. C. G.; Braune, B. M. Prevalence of long-chained perfluorinated carboxylates in seabirds from the canadian arctic between 1975 and 2004. *Environmental Science & Technology* **2007**, *41* (10), 3521-3528. DOI: 10.1021/es062710w.

(18) Leat, E. H. K.; Bourgeon, S.; Eze, J. I.; Muir, D. C. G.; Williamson, M.; Bustnes, J. O.; Furness, R. W.; Borga, K. Perfluoroalkyl substances in eggs and plasma of an avian top predator, great skua (Stercorarius skua), in the north Atlantic. *Environmental Toxicology and Chemistry* **2013**, *32* (3), 569-576. DOI: 10.1002/etc.2101.

(19) Blevin, P.; Angelier, F.; Tartu, S.; Bustamante, P.; Herzke, D.; Moe, B.; Bech, C.; Gabrielsen, G. W.; Bustnes, J. O.; Chastel, O. Perfluorinated substances and telomeres in an Arctic seabird: Cross-sectional and longitudinal approaches. *Environmental Pollution* **2017**, *230*, 360-367. DOI: 10.1016/j.envpol.2017.06.060.

(20) Munoz, G.; Labadie, P.; Geneste, E.; Pardon, P.; Tartu, S.; Chastel, O.; Budzinski, H. Biomonitoring of fluoroalkylated substances in Antarctica seabird plasma: Development and validation of a fast and rugged method using on-line concentration liquid chromatography tandem mass spectrometry. *Journal of Chromatography A* **2017**, *1513*, 107-117. DOI: 10.1016/j.chroma.2017.07.024.

(21) Svendsen, N. B.; Herzke, D.; Harju, M.; Bech, C.; Gabrielsen, G. W.; Jaspers, V. L. B. Persistent organic pollutants and organophosphate esters in feathers and blood plasma of adult kittiwakes (Rissa tridactyla) from Svalbard - associations with body condition and thyroid hormones. *Environ Res* **2018**, *164*, 158-164. DOI: 10.1016/j.envres.2018.02.012.

(22) Roscales, J. L.; Vicente, A.; Ryan, P. G.; Gonzalez-Solis, J.; Jimenez, B. Spatial and Interspecies Heterogeneity in Concentrations of Perfluoroalkyl Substances (PFASs) in Seabirds of the Southern Ocean. *Environmental Science & Technology* **2019**, *53* (16), 9855-9865. DOI: 10.1021/acs.est.9b02677.

(23) Jones, P. D.; Hu, W.; De Coen, W.; Newsted, J. L.; Giesy, J. P. Binding of perfluorinated fatty acids to serum proteins. *Environ. Toxicol. Chem.* **2003**, *22* (11), 2639-2649. DOI: https://doi.org/10.1897/02-553.

(24) Forsthuber, M.; Kaiser, A. M.; Granitzer, S.; Hassl, I.; Hengstschläger, M.; Stangl, H.; Gundacker, C. Albumin is the major carrier protein for PFOS, PFOA, PFHxS, PFNA and PFDA in human plasma. *Environment International* **2020**, *137*, 105324. DOI: https://doi.org/10.1016/j.envint.2019.105324.

(25) Li, S.; Cao, Y.; Geng, F. Genome-Wide Identification and Comparative Analysis of Albumin Family in Vertebrates. *Evolutionary Bioinformatics* **2017**, *13*, 1176934317716089. DOI: 10.1177/1176934317716089.

(26) Bangma, J.; Guillette, T. C.; Bommarito, P. A.; Ng, C.; Reiner, J. L.; Lindstrom, A. B.; Strynar, M. J. Understanding the dynamics of physiological changes, protein expression, and PFAS in wildlife. *Environment International* **2022**, *159*, 107037. DOI: https://doi.org/10.1016/j.envint.2021.107037.

(27) Alesio, J. L.; Slitt, A.; Bothun, G. D. Critical new insights into the binding of poly- and perfluoroalkyl substances (PFAS) to albumin protein. *Chemosphere* **2022**, *287*, 131979. DOI: https://doi.org/10.1016/j.chemosphere.2021.131979.

(28) Martin, J. W.; Mabury, S. A.; Solomon, K. R.; Muir, D. C. G. Bioconcentration and tissue distribution of perfluorinated acids in rainbow trout (Oncorhynchus mykiss). *Environmental Toxicology and Chemistry* **2003**, *22* (1), 196-204. DOI: https://doi.org/10.1002/etc.5620220126.

(29) Giesy, J. P.; Kannan, K. Global Distribution of Perfluorooctane Sulfonate in Wildlife. *Environ. Sci. Technol.* **2001**, *35* (7), 1339-1342. DOI: 10.1021/es001834k.

(30) Houde, M.; De Silva, A. O.; Muir, D. C. G.; Letcher, R. J. Monitoring of Perfluorinated Compounds in Aquatic Biota: An Updated Review. *Environ. Sci. Technol.* **2011**, *45* (19), 7962-7973. DOI: 10.1021/es104326w.

(31) Hobson, K. A.; Clark, R. G. Turnover of ^{13}C in Cellular and Plasma Fractions of Blood: Implications for Nondestructive Sampling in Avian Dietary Studies. *The Auk* **1993**, *110* (3), 638-641. DOI: 10.2307/4088430 (acccessed 2023/11/13/).JSTOR.

(32) Newsted, J. L.; Coady, K. K.; Beach, S. A.; Butenhoff, J. L.; Gallagher, S.; Giesy, J. P. Effects of perfluorooctane sulfonate on mallard and northern bobwhite quail exposed chronically via the diet. *Environmental Toxicology and Pharmacology* **2007**, *23* (1), 1-9. DOI: https://doi.org/10.1016/j.etap.2006.04.008.

(33) Yoo, H.; Guruge, K. S.; Yamanaka, N.; Sato, C.; Mikami, O.; Miyazaki, S.; Yamashita, N.; Giesy, J. P. Depuration kinetics and tissue disposition of PFOA and PFOS in white leghorn chickens (Gallus gallus) administered by subcutaneous implantation. *Ecotox Environ Safe* **2009**, *72* (1), 26-36. DOI: https://doi.org/10.1016/j.ecoenv.2007.09.007.

(34) Seacat, A. M.; Thomford, P. J.; Hansen, K. J.; Olsen, G. W.; Case, M. T.; Butenhoff, J. L. Subchronic Toxicity Studies on Perfluorooctanesulfonate Potassium Salt in Cynomolgus Monkeys. *Toxicological Sciences* **2002**, *68* (1), 249-264. DOI: 10.1093/toxsci/68.1.249 (acccessed 11/13/2023).

(35) Hekster, F.; De Voogt, P.; Pijnenburg, A.; Laane, R. *Perfluoroalkylated substances: Aquatic environmental assessment*; Rijkswaterstaat, RIKZ, 2002.